ERJ Express. **Published on November 14, 2008 as doi: 10.1183/09031936.00014808**

Amifostine reduces lung vascular permeability via suppression of inflammatory signaling.

Panfeng Fu[1], Anna A. Birukova[1], Junjie Xing[1], Saad Sammani[1], Jeffrey S. Murley[2], Joe G.N. Garcia[1], David J. Grdina[2], Konstantin G. Birukov[1]

[1] Section of Pulmonary and Critical Care Medicine, Department of Medicine and [2]Department of Radiation and Cellular Oncology, University of Chicago, Chicago, Illinois 60637

Correspondence and requests of reprints should be addressed to Konstantin Birukov, MD, PhD

Corresponding address:
Konstantin G. Birukov
Section of Pulmonary and Critical Care Medicine
Department of Medicine
University of Chicago
929 E. 57th Street, GCIS Bldg, Room W410
Chicago, IL 60637
Phone: (773) 834-2636
Fax: (773) 834-2683
e-mail: kbirukov@medicine.bsd.uchicago.edu

Running head: amifostine and LPS-induced endothelial leak

Word count: 4443

Copyright 2008 by the European Respiratory Society.

Abstract

Despite encouraging outcome of antioxidant therapy in animal models of acute lung injury, effective antioxidant agents for clinical application remain to be developed. We studied the effect of pretreatment with thiol antioxidant compound, amifostine, on lung endothelial barrier dysfunction induced by gram-negative bacteria wall lipopolysaccharide.

Endothelial permeability was monitored by changes in transendothelial electrical resistance. Cytoskeletal remodeling and reactive oxygen species production was examined by immunofluorescence. Cell signaling was assessed by western blot. Measurements of Evans blue extravasation, cell count and protein content in bronchoalveolar lavage fluid were used as *in vivo* parameters of lung vascular permeability.

Hydrogen peroxide, lipopolysaccharide, and interleukin-6 caused cytoskeletal reorganization and increased permeability in the pulmonary endothelial cells reflecting endothelial barrier dysfunction. These disruptive effects were inhibited by pretreatment with amifostine and linked to the amifostine-mediated abrogation of ROS production and redox-sensitive signaling cascades including p38, Erk1/2 MAP kinases, and $NF_{\kappa}B$ pathway. *In vivo*, concurrent amifostine administration inhibited LPS-induced oxidative stress and p38 MAP kinase activation, which was associated with reduced vascular leak and neutrophil recruitment to the lungs.

These studies demonstrate for the first time protective effects of amifostine against lipopolysaccharide-induced lung vascular leak in vitro and in animal models of LPS-induced acute lung injury.

Keywords: endothelium, lung, lipopolysaccharide, permeability, reactive oxygen species

Introduction

Activation of tissue inflammation, oxidant-mediated tissue injury, and increased vascular leak are cardinal features in the pathogenesis of acute lung injury (ALI) and the more severe acute respiratory distress syndrome. In this condition, reactive oxygen and nitrogen species (ROS and RNS) produced by lung cells can oxidize and nitrate key lung proteins and phospholipids and inhibit their functions, or they may activate redox-sensitive pathological signaling pathways. Pro-inflammatory stimuli such as bacterial wall lipopolysacharide (LPS), tumor necrosis factor-α (TNF-α), and interleukin -1 are potent triggers of lung inflammatory response. These same stimuli also elicit an oxidative cellular stress response [1, 2]. An extensive body of evidence shows a crosstalk between the cellular signaling pathways and the cellular redox state through multiple mechanisms. For example, generation of ROS, such as H_2O_2, leads to activation of protein tyrosine kinases, mitogen-activated protein kinases, and their downstream effectors [3]. However, ROS may also damage cells. At sites of inflammation and infection, the local cellular environment is enriched with ROS, cytokines, and chemokines. Besides bactericide action, ROS can also attack and damage host tissues, and thus contribute to the pathogenesis of acute respiratory distress syndrome, reperfusion injury and other diseases. Levels of ROS/RNS correlate with the outcome of the disease and the severity of injury to the vascular endothelium and alveolar epithelium. Although the potential role of antioxidant enzymes and scavengers of ROS/RNS in reducing the severity of ALI has been recognized, the search for potential protective

compounds continues; and animal and cell culture models for testing potential therapeutic compounds in ALI setting are yet to be developed.

Amifostine (S-2[3-aminopropylamino]- ethylphosphorothioic acid, WR-2721) is a phosphorothioate that is converted to its active free thiol form by dephosphorylation by alkaline phosphatase in tissue. It has been approved by the FDA for use as a cytoprotective agent to decrease the incidence of moderate-to-severe xerostomia in patients undergoing postoperative radiation therapy for the treatment of head-and-neck cancer [4]. As a reducing agent capable of participating in intracellular reductive/oxidative process, amifostine has the potential to affect redox-sensitive transcription factors and gene expression once inside the cell [5]. Therefore, previous studies of amifostine focused on its radioprotective effects in tumor radiotherapy, where it acts as an oxidant scavenger. However, although recent studies have demonstrated potential role of amifostine in pulmonary protection against bleomycin- or radiation-induced pulmonary toxicity [6, 7], it has not been tested yet as potential protective therapy against sepsis and endotoxin-induced acute lung injury. Compound WR-2721 is a stable but inactive precursor of WR-1065. When injected, WR-2721 is modified by membrane-bound alkaline phosphatase highly expressed in the endothelium, and transferred into the bioactive thiol metabolite WR-1065, which quickly penetrates into cell, where the thiol groups act as free-radical scavengers and protect cells from oxidative damage. On the other hand, the endothelium is a major source of oxidants and may contribute to the oxidant-rich environment at the inflammatory locus.

The aim of this study was to test effects of FDA approved compound amifostine against EC barrier dysfunction induced by LPS and inflammatory cytokines in vitro and test its efficiency as pretreatment in preventing the endotoxin-induced acute lung injury in mouse model. Our results suggest that the protective effect of amifostine may be mediated by its antioxidant properties resulting in downregulation of oxidative stress and redox-sensitive signaling cascades which lead to attenuation of lung vascular leak.

Materials and Methods

Reagents and cell culture. Unless otherwise specified, all reagents including β-actin antibodies (catalog # A-5441) were obtained from Sigma (St. Louis, MO). Amifostine compounds WR-1065 (free thiol form used for cell culture experiments) and WR-2721 (prodrug formulation used *in vivo* experiments) were obtained from the Drug Synthesis and Chemistry Branch, Division of Cancer Treatment, National Cancer Institute. Interleukin-6 (IL-6) and IL-6 soluble receptor (SR) were obtained from R&D Systems (Minneapolis, MN). VE-cadherin antibodies (catalog # sc-9989) were purchased from Santa Cruz Biotechnology (Santa Cruz, CA), nitrotyrosine antibodies (catalog # 32-1900) were purchased from Invitrogen (San Francisco, CA), antibodies against phosphorylated MLC (catalog # 3674), p38 (catalog # 9216), Hsp27 (catalog # 2401), MEK1/2 (catalog # 9121), Erk1/2 (catalog # 9101), IκBα (catalog # 9246), and NFκB-p65 (catalog # 3031) were obtained from Cell Signaling (Beverly, MA). All reagents used for immunofluorescence staining were purchased from Molecular Probes (Eugene, OR). Human pulmonary artery endothelial cells (HPAEC) were obtained from Clonetics (Walkersville, MD), cultured according to the manufacturer's protocol, and used at passages 5-9.

Endothelial cell imaging. EC monolayers grown on glass coverslips were stimulated with agonist of interest, then washed with room temperature PBS twice and fixed in 3.7% paraformaldehyde solution in PBS for 10 min at room temperature followed by double immunofluorescence staining with Texas Red-conjugated phalloidin to visualize actin filaments and VE-cadherin antibody to

visualize EC adherens junctions. EC cytoskeletal organization was analyzed as we have previously described [8].

Measurements of transendothelial electrical resistance. The cellular barrier properties were analyzed by measurements of transendothelial electrical resistance across confluent endothelial cell monolayers using the electrical cell-substrate impedance sensing system (Applied Biophysics, Troy, NY). Cells were cultured on small gold electrodes (10^{-4} cm^2), and culture media was used as electrolyte. The total electrical resistance was measured dynamically across the monolayer using an electrical cell-substrate impedance sensing system (ECIS) (Applied Biophysics, Troy, NY) and was determined by the combined resistance between the basal surface of the cell and the electrode, reflective of focal adhesion, and the resistance between the cells, as described previously as previously described [8].

Detection of ROS production in live cells. ROS production was measured using Image-iT LIVE Green Reactive Oxygen Species Detection Kit (Molecular Probes, Inc., Eugene, OR, USA). Confluent EC monolayers grown in 12-well plate were pretreated with unprotected form of amifostine (WR-1065, 4 mM, 30 min) or N-acetylcysteine (NAC, 5 mM, 1 hr) followed by LPS stimulation for 6 hrs. After stimulation, cells were washed in 37 °C Hanks buffer and incubated with 1 ml of 25 μM carboxy-H2DCFDA working solution (25 min, 37 °C, protected from light). After 3-time wash in warm Hanks buffer cells were subjected to microscopy using Nikon video-imaging system (Nikon Inc, Tokyo,

Japan) consisting of phase contrast inverted microscope equipped with set of objectives and filters for immunofluorescence and connected to a digital camera and image processor. Ten fields were randomly chosen for each experiment condition. Immunofluorescence signal intensity was measured and expressed in arbitrary units per microscopic field.

Western blot analysis. Protein extracts from mouse lungs or EC lysates were separated by SDS-PAGE and transferred onto nitrocellulose membranes followed by incubation with specific antibodies of interest. Equal protein loading was verified by re-probing of membranes with anti-β-actin antibody. Immunoreactive proteins were detected using the enhanced chemiluminescent detection system according to the manufacture's protocol (Amersham, Little Chalfont, UK). The relative intensities of immunoreactive protein bands (RDU) were quantified by scanning densitometry using Image Quant software (Molecular Dynamics, Sunnyvale, CA).

***In vivo* model of ALI**. Adult male C57BL/6J mice, 8-10 week old, with average weight 20-25 grams (Jackson Laboratories, Bar Harbor, ME) were anesthetized with an intraperitoneal injection of ketamine (75 mg/kg) and acepromazine (1.5 mg/kg) according. LPS (0.7 mg/kg body weight, Escherichia coli O55:B5, dissolved in sterile water) or sterile water was injected intratracheally in a small volume (20-30 μl) using a 20 gauge catheter Penn-Century Inc., (Philadelphia, PA). Although water is a hypotonic solvent, it did not induce any noticeable injury

in control animals injected with 20 μl sterile water, when compared with untreated mice or mice injected with 20 μl normotonic physiologic solution (data not shown). Mice were randomized to concurrently receive sterile saline solution or amifostine (WR-2721, 200 mg/kg) by intraperitoneal injection to yield the experimental groups: control, LPS (0.7 mg/kg) only, WR-2721 (200 mg/kg) only, and LPS (0.7 mg/kg) + WR-2721 (200 mg/kg). All animal experiments were approved by the University of Chicago Institutional Animal Care & Use Committee for the humane treatment of experimental animals.

Bronchoalveolar lavage fluid (BAL) analysis. After 18 hrs, animals were sacrificed by exsanguination under anesthesia. Tracheotomy was performed, and the trachea was cannulated with a 20 gauge intravenous catheter, which was tied into place. BAL was performed using 1 ml of warmed sterile Hanks Balanced Salt Buffer (+30°C). The collected lavage fluid was centrifuged at 2500 rpm for 20 min at +4°C; the supernatant was removed and frozen at –80°C for subsequent protein study. The cell pellet was then resuspended in 1 ml of red blood cell lysis buffer (ACK Lysing Buffer, Invitrogen, Carlsbad, CA) for 5 min. Red blood cell lysis buffer was used to eliminate red cells from the cell pellet, because presence of a large number of red cells in cell suspension may compromise counting of white cells. White cells were then re-pelleted by centrifugation at 2500 rpm for 20 min at +4°C. The cell pellet was again resuspended in 200 μl of PBS, and 20 μl aliqouts were taken for cell counting using hemocytometer. In brief, 20 μl of cell suspension was mixed with 20 μl of Trypan blue and allowed to sit in the room temperature for 5 min. Cells were

loaded onto a hemocytometer and then counted under a microscope. The remaining 180 µl of cell suspension were re-pelleted by centrifugation, and cell pellets were stored at -80°C for subsequent detection of myeloperoxidase activity (MPO). The BAL protein concentration was determined by Bio-Rad DC protein assay kit (Bio-Rad Laboratories, Hercules, CA), which allows the reaction to reach 90% of its maximum color development within 15 min and the color changes not more than 5% in 1 hour. The absorbance was measured at 750 nm, and protein concentration was determined using standard curves.

Assessment of pulmonary vascular leakage by Evans blue. Evans blue dye (EBD, 30 ml/kg) was injected into the external jugular vein 2 hrs before termination of experiment to assess vascular leak. In brief, at the end of experiment, thoracotomy was performed, and the lungs were perfused free of blood with PBS containing 5 mM EDTA. Left lung and right lungs were excised and imaged by Kodak digital camera. After imaging, lungs were blotted dry, weighed and homogenized in PBS (1 ml /100 µg tissue) and used for quantitative analysis of EB tissue accumulation as described elsewhere [9]. Briefly, homogenized tissue was incubated with 2 volumes of formamide (18 h, 60°C) and centrifuged at 12,000 g for 20 min. Optical density of the supernatant was determined by spectrophotometry at 620 nm and 740 nm. EBD concentration in the lung tissue homogenates (µg Evans blue dye / g tissue) was calculated against a standard curve.

Histological assessment of lung injury. Left lungs were intratracheally instilled with 10% formalin from 20 cm height, immersed in 10% formalin for at least 24 hours and then embedded in paraffin. After deparaffinization and dehydration, the lungs were cut into 4-μm sections, and stained with hematoxylin and eosin. Alveolar fluid accumulation and neutrophil infiltration as indices of lung leak and inflammation were evaluated by bright field microscopy of lung tissue sections at x 40 magnification.

Statistical analysis. Results are presented as mean ± SD of three to ten independent experiments. Stimulated samples were compared to controls by unpaired Student's t-test. For multiple-group comparisons, a one-way variance analysis (ANOVA), followed by the post hoc Fisher's test, were used. $P<0.05$ was considered statistically significant.

Results

Role of amifostine in prevention of inflammatory agonist-induced hyper-permeability. To test the hypothesis that a radiation protection compound with antioxidant properties, amifostine, may attenuate lung endothelial hyper-permeability induced by inflammatory agents, we examined effects of amifostine on endothelial permeability induced by LPS and inflammatory cytokine IL-6. EC treatment with H_2O_2 was used as an LPS-independent control for oxidative stress. Pretreatment of human pulmonary EC monolayers with a cell permeable free thiol form of amifostine, WR-1065, (0.4 – 4.0 mM) significantly attenuated H_2O_2–induced EC permeability judged by marked decrease of transendothelial electrical resistance (**Figure 1A**). Maximal protective effect of amifostine was achieved at the concentration 4 mM. Similarly, amifostine alone did not affect basal TER, but inhibited EC hyper-permeability induced by LPS (**Figure 1B**). Amifostine at 4 mM is routinely used for *in vitro* studies and demonstrates cytoprotective effects without side effects [10]. For comparision, the NAC concentrations used *in vitro* were in the 10-20 mM range [11, 12].

We have previously shown activation of IL-6 production in the lungs induced by LPS intratracheal instillation [8]. In vitro, combination of IL-6 and its soluble receptor (SR) increases pulmonary EC permeability [13]. Pretreatment of EC with amifostine significantly reduced TER increases in response to (IL-6 + SR) challenge (**Figure 1C**). Taken together, these data strongly suggest a protective effect of amifostine pretreatment against EC barrier dysfunction induced by inflammatory agonists.

Effects of amifostine on endothelial cytoskeletal remodeling and disruption of adherens junctions induced by inflammatory agonists. In the following experiments we assessed effects of amifostine on cytoskeletal remodeling and disruption of adherens junctions caused by H_2O_2, LPS and IL-6 with its soluble receptor (IL-6 + SR) and associated with endothelial barrier compromise. After agonist challenge, cytoskeletal remodeling and integrity of adherens junctions in control and amifostine-pretreated pulmonary EC were examined by immunostaining for F-actin and VE-cadherin. In unstimulated cells and cells treated with amifostine alone, F-actin was primarily organized into actin bundles randomly distributed in the cell (**Figure 2A**). Upon stimulation with H_2O_2, LPS, or IL-6 + SR, F-actin was reorganized into thicker stress fibers in the center of the cells. These changes were associated with appearance of paracellular gaps (shown by arrows) indicating EC barrier compromise. Remarkably, amifostine pretreatment attenuated agonist-induced stress fibers and gap formation. In agreement with these data, pre-incubation of pulmonary EC with amifostine also attenuated H_2O_2- and LPS-induced disruption of monolayer integrity, as detected by immunofluorescence staining for VE-cadherin (**Panel B,** shown by arrows). These results suggest that the protective role of amifostine may be attributed to its ability to attenuate cytoskeletal remodeling induced by H_2O_2, LPS, and IL-6. These results show that protective effects of amifostine against H_2O_2-, LPS-, or IL-6-induced hyper-permeability are also associated with preservation of cytoskeletal and cell-cell junction organization.

Effects of amifostine on ROS production induced by LPS. To test the hypothesis that amifostine may attenuate LPS-induced EC cytoskeletal remodeling and barrier dysfunction by its ability to scavenge ROS, we measured ROS production in the EC stimulated with LPS with or without amifostine pretreatment. An anti-oxidant N-acetyl cysteine (NAC) was used as a positive control. LPS treatment (6 hrs) increased ROS production in pulmonary EC in a dose-dependent manner with maximal effect at 500 ng/ml LPS (**Figure 3**). Pretreatment with amifostine or NAC significantly reduced ROS production by LPS. Importantly, amifostine was more effective in suppression of LPS-induced ROS production. These results suggest that the protective role of amifostine in preventing H_2O_2-, LPS-, or (IL-6 + SR)-induced EC barrier dysfunction may be mediated at least in part by its antioxidant activity.

Regulation of oxidative stress-sensitive signaling molecules by amifostine. ROS and associated oxidative stress are shown to activate various signaling molecules, such as Erk-1/2, p38, JNK MAP kinases, and NF-$_K$B signaling, which are intimately involved in control of EC permeability and inflammation and regulated by phosphorylation on serine/threonine and tyrosine residues.

In the next series of experiments we investigated effects of amifostine on the regulation of MAPK- and NF-$_K$B-dependent signaling activated by oxidative stress. Western blot analysis of pulmonary EC stimulated with or without amifostine pretreatment showed that amifostine abolished LPS-, IL-6-, and H_2O_2-induced activation of Erk-1,2 and p38 MAPK cascades (**Figure 4**), as detected by phosphorylation of MEK1/2, Erk1/2, p38 MAPKs, and p38-

dependent regulator of actin dynamics Hsp27. Amifostine dramatically attenuated LPS-induced phosphorylation of IκBα and NFκB p65 subunit (**Figure 4A**), which are critical for activation of NFκB-dependent transcription. Similar results were obtained in EC monolayers stimulated with H_2O_2 (**Figure 4B**).

Increased myosin light chain (MLC) phosphorylation is associated with increased actin polymerization and activation of actomyosin contraction. Additionally, inflammatory mediators may inactivate myosin-associated protein phosphatase [14] and thus further promote MLC phosphorylation, a marker of endothelial cell contraction. In the following experiments we analyzed effects of amifostine on phosphorylation of MLC induced by LPS, IL-6, or H_2O_2. Pretreatment with amifostine significantly inhibited phosphorylation of MLC induced by these agonists (**Figure 4, lower panels**), which is consistent with protective effects of amifostine on the EC barrier under oxidative stress and inflammatory stimulation.

Taken together, the results of cell culture experiments strongly suggest that the activation of p38, Erk-1/2 MAPK, and NFκB pathways are associated with EC stress responses to inflammatory agonists, and indicate a potent protective effect of amifostine against EC oxidative stress, barrier dysfunction, and cytoskeletal remodeling.

Effects of amifostine on LPS-induced cell infiltration in mouse lungs. To evaluate a role of amifostine in the modulation of lung permeability, we used *in vivo* model of LPS-induced acute lung injury. The pro-drug form of amifostine was used in the in *vivo* studies. LPS induced dramatic lung injury with a nearly

10-fold increase in BAL cell counts at 18 hours (2.52 ± 0.76 X 10^5 cells/ml versus 2.46 ± 0.33 X 10^6 cells/ml, $p<0.001$) (**Figure 5A**). The influx of neutrophils into the lungs in response to LPS was inhibited by treatment with amifostine (2.46 ± 0.33 X 10^6 cells/ml versus 1.22 ± X 0.24 x10^6 cells/ml, $p<0.001$). Correspondingly, the activity of myeloperoxidase, a marker of tissue oxidative stress and inflammation induced by activated neutrophils, was dramatically decreased by amifostine pretreatment, as compared to LPS alone (37 ± 8.5 U/ml versus 148.3 ± 61.4 U/ml, $p<0.01$) (**Figure 5B**).

Histological analysis of lung paraffin-embedded lung tissue sections stained with hematoxyllin and eosin was performed to further examine effects of amifostine on LPS-induced changes in lung microstructure. LPS stimulation (18 hrs) induced significant neutrophil accumulation in the lung parenchyma, which was significantly reduced by amifostine treatment (**Figure 5C**). These results clearly demonstrate that amifostine may inhibit LPS-induced acute lung injury.

Effects of amifostine on LPS-induced lung vascular leak. In the following studies, we examined effects of amifostine on LPS-induced lung vascular leak. Analysis of BAL protein content was used as an index of lung vascular permeability. Intratracheal instillation of LPS significantly increased in the total protein concentration in BAL fluid (**Figure 6A**), as compared to control animals (0.14 ± 0.04 mg/ml versus 1.01 ± 0.13 mg/ml, $p<0.001$). Concurrent treatment with LPS and amifostine significantly attenuated BAL protein concentrations, in comparison to LPS alone (0.46 ± 0.12 mg/ml versus 1.01 ± 0.13 mg/ml,

p<0.001). There was no significant difference in BAL protein in amifostine-treated animals and controls in the absence of LPS.

The protective effects of amifostine against LPS-induced lung vascular barrier compromise were further assessed by measurement of Evans blue leakage into the lung tissue. LPS caused substantial Evans blue leakage from the vascular space into the lung parenchyma, which was significantly decreased by amifostine treatment (**Figure 6B**). These results were confirmed by quantitative analysis of Evans blue-labeled albumin extravagation in the lung preparations (**Figure 6C**). Evans blue accumulation in the lungs from LPS-treated mice was significantly increased (16.95 ± 3.46 μg/g wet weight lung versus 6.63 ± 0.40 μg/g wet weight lung in non-treated controls, p<0.001). LPS-induced tissue accumulation of Evans blue was reduced by amifostine treatment (8.77 ± 1.48 μg/g wet weight lung vs. 16.95 ± 3.46 μg/g wet weight lung, p<0.001). Thus, our data demonstrate protective effects of amifostine in the mouse model of vascular permeability induced by LPS.

Effects of amifostine on LPS-induced oxidative stress-sensitive signaling *in vivo*. We next examined whether the protective effect of amifostine *in vivo* was associated with its antioxidant properties. LPS-induced ROS production, NO synthase activation and increased NO generation leads to rapid reaction of NO with superoxide and generation of peroxynitrite [15] leading to nitration of protein tyrosine residues. Thus, the presence of proteins with nitrated tyrosine residues can be used as a marker of oxidative stress *in vivo* including ARDS [16]. We performed western blot analysis of lung tissue samples from LPS- and

amifostine+LPS-treated mice to detect the presence of tyrosine nitrated proteins. LPS treatment increased the content of nitrotyrosine-containing proteins in the lung tissue samples with major bands observed in the 25 kDa and 50 kDa range, which was significantly attenuated by amifostine treatment (**Figure 7A, upper panel**). After 6 hrs of LPS challenge, nitrotyrosine-containing proteins were mainly detected in the 50 kDa range. Amifostine pretreatment significantly decreased LPS-induced protein nitration. In addition, amifostine dramatically attenuated LPS-induced phosphorylation of p38 MAPK (**Figure 7A, middle panel**). These results strongly suggest that the protective effect of amifostine *in vivo* is associated with the reduction of LPS-induced oxidative stress and redox-sensitive stress kinase signaling.

The following experiments tested a dose dependence of amifostine protective effects in the LPS model of lung vascular leak. Amifostine exhibited protective effects against LPS-induced increases in the BAL cell count (**Figure 7B**) and protein content (**Figure 7C**) in the 25 – 200 mg/kg dose range. Remarkably, even low doses of amifostine (25 mg/ kg) exhibited nearly maximal protective effect against BAL protein accumulation, although maximal suppression of BAL cell accumulation was achieved at 200 mg/kg amifostine.

Discussion

Although ROS generated under physiologic conditions play an important role in cell homeostasis and cell signal transduction [17], their excessive generation at sites of inflammation becomes detrimental and may cause tissue injury. The vascular endothelium, which regulates the passage of macromolecules and circulating cells from blood to tissue, becomes readily exposed to oxidative stress and plays a critical role in the pathophysiology of several vascular disorders. This study demonstrated that amifostine, which acts as a donor of active free thiol, inhibited LPS-induced endothelial monolayer disruption and attenuated LPS-induced lung vascular leak via downregulation of ROS and tissue oxidative stress.

LPS is an important trigger of the lung inflammation involved in pathogenesis of lung edema and ARDS. Through binding to its receptor, CD14, on the cell membrane, LPS induces the release of proinflammatory cytokines. As a result of LPS challenge, activated neutrophils migrate into the lung interstitium from the blood circulation and produce significant amounts of ROS leading to further escalation of inflammation. Activated endothelial cells may be another important source of ROS contributing to the formation of oxidant-rich environment at the sites of inflammation. Our results show significant ROS production by pulmonary EC induced by LPS. Furthermore, H_2O_2-, LPS- and IL-6-induced stress fiber formation and disruption of adherens junctions in pulmonary EC monolayers was prevented by amifostine. The barrier protective effect of amifostine observed in this study was linked to its ability to inhibit ROS

production and attenuate redox-dependent pro-inflammatory signaling in the EC cultures and in the murine model of LPS-induced acute lung injury.

NFkB is a redox-sensitive transcription factor activated upon LPS stimulation, which triggers inflammatory signaling and activates expression of proinflammatory cytokines. Our data show that potent inhibitory effects of amifostine pretreatment on the LPS-induced NFkB activation. Erk-1,2 and p38/MK-2 MAP kinase pathways and NF-kB may become activated in a redox-sensitive manner [3]. In addition, p38 MAPK may be involved in actin filament reorganization in response to oxidative stress via MAPK-dependent phosphorylation of actin-binding effector Hsp27. This study shows that phosphorylation of p38 and Hsp27 caused by LPS or H_2O_2 was attenuated by amifostine *in vitro* and *in vivo*. In addition, amifostine pretreatment abolished LPS-, H_2O_2-, and IL-6-induced activation of regulatory MLC, which triggers EC contraction and barrier dysfunction. Inflammatory cytokine IL-6 is a marker of inflammation elevated in the model of endotoxin-induced lung injury [8, 18]. Soluble IL-6 receptor (SR) is a 50-55 kDa ligand binding protein, which can bind its ligand and induce cellular responses by association with gp130, thus acting as an IL-6 agonist. The association of IL-6 with the soluble form of SR-alpha is capable of eliciting a biological response in cells that express only the membrane gp130. We have previously described that single treatment of HPAEC with IL-6 or its soluble receptor did not significantly change basal TER levels, whereas combination of IL-6 and SR induced significant TER decrease [13]. In the current study we used combined IL-6 and its soluble receptor treatment to reproduce inflammatory reactions in pulmonary endothelium. In

these experiments, IL6/SR-induced EC barrier dysfunction, cytoskeletal remodeling and phosphorylation of p38 MAPK target, HSP27, (Figures 1,2,4) was attenuated by amifostine. Collectively, these results demonstrate that the LPS-induced oxidative stress plays essential role in activation of inflammatory signaling and cytoskeletal remodeling leading to EC permeability and lung vascular leak, which can be markedly attenuated by amifostine pretreatment.

Western blot detection of nitrotyrosinated proteins, a footprint of oxidative stress, showed increased lung tissues levels of nitrotyrosinated protein immunoreactivity after 2 hrs and 6 hrs of LPS exposure, which were markedly attenuated by amifostine (Figure 8). Antioxidant strategies for attenuation of lung inflammatory injury have been tested in previous studies. For example, N-acetyl cysteine (NAC), a thiol antioxidant compound, exhibited antioxidant effects and suppressed ROS-mediated lung injury [19]. Similar to amifostine, NAC attenuated activation of p38 and MKK3/MKK6 in the TNFα model of EC barrier dysfunction [20]. However, NAC application in clinical settings did not prove its efficiency. In fibrous alveolitis, where activated inflammatory cells induce oxidative stress in a lower respiratory tract, high doses of NAC (1.8 g daily for 12 weeks in addition to immunosuppressive therapy) did not significantly suppress inflammatory cell activation [21]. A Nordic Multi-Centre Controlled Trial showed that a 6-day course of intravenous NAC during the first week of life does not prevent bronchopulmonary dysplasia or death, or improve lung function at term in infants with extremely low birth weight [22]. Although previous studies demonstrated protective effects of amifostine on radiation- or chemotherapy-induced acute lung toxicity, there is no direct evidence of amifostine protective

effect in the model of endotoxin-induced acute lung injury. Our results indicate potent protective effects of amifostine against LPS-induced pulmonary EC barrier compromise *in vitro* and LPS-induced lung leukocyte infiltration, BAL protein accumulation and vascular leak. Amifostine inhibited LPS-induced leukocyte accumulation in the BAL in a dose-dependent manner. Maximum protective effect achieved at 200 mg/kg. However, marked protective effects were still observed at significantly lower dose (25 mg/kg), which does not cause toxic side effects. A dose of 910 mg/m^2 amifostine was originally established for use in clinical chemotherapy studies. At this concentration side effects including nausea, vomiting hypotension, and hypocalcemia were noticed. In the current study the protective effects of amifostine against lung injury were observed even at substantially lower doses of amifostine without introducing side effects. These results suggest a potential utilization of amifostine as clinical treatment of acute lung injury syndromes. Another advantage of amifostine over other antioxidants including NAC is comparable efficiency at different routes of administration. For the most antioxidant agents, the maximal effect is usually achieved by intravenous injection. In contrast, amifostine exhibits comparable effects during subcutaneous and intravenous [23], as well as intraperitoneal [24] administration.

Several lines of evidence suggest that endothelium is a major site of amifostine absorbance and conversion to active form. WR-2721 is presumably modified by membrane-bound alkaline phosphatase, which is highly expressed in the endothelium, and transferred into the thiol metabolite WR-1065, which quickly penetrates into cell, where the thiol groups act as free-radical

scavengers and protect cells from oxidative damage [25]. On the other hand, pulmonary endothelium and epithelium are the major sources of oxidants in the lung and possibly significant contributors in maintaining the oxidant-rich environment at the inflammatory locus. Based on our data, we speculate that the potent protective effects of amifostine in the LPS-induced vascular leak may be attributed to its local activation by lung microvascular endothelium in the inflamed lungs leading to increased capacity to prevent lung microvascular endothelium and alveolar epithelium from attack by oxidants.

Amifostine is a negative charged thiol, as compared to the neutral charge of NAC, which allows amifostine accumulation within the mitochondria and around the negatively charged DNA. This effect is called the net charge of thiols model. Negatively charged thiols possess higher protective potential than neutral or positively charged thiols [26]. Indeed, amifostine exhibited direct and more potent than NAC cytoprotective effects in cells during radiation exposure [27]. The second protective mechanism of amifostine and NAC action is ability to activate NFkB by virtue of their SH group and enhance gene expression of intracellular anti-oxidant enzyme MnSOD. Amifostine exhibits higher efficiency in stimulating MnSOD expression than NAC on an equal molar basis [5]. As a result, this activation leads to enhanced resistance for radiation-induced ROS and may also contribute to reduction of oxidative stress in chronic inflammatory lung injury. These findings strongly suggest that amifostine may exhibit more potent, than NAC protective effects in the clinical settings associated with pathologic ROS production accompanying LPS-induced lung injury. In contrast to NAC, amifostine is approved by FDA for a radioprotective and cytoprotective

treatment in the course of radiation therapy treatments. These features make amifostine more attractive compound for potential clinical testing.

In summary, these studies show potent protective effects of amifostine pre-treatment in the models of LPS-induced lung injury *in vivo* and pulmonary EC barrier dysfunction *in vitro* via attenuation of oxidative stress, inhibition of redox-sensitive MAP kinases, NF-kB inflammatory cascade, and attenuation of LPS-induced cytoskeletal remodeling and disruption of endothelial cell adhesions leading to preservation of EC monolayer integrity (**Figure 8**). Amifostine is currently used as a cytoprotective compound against the toxic effects of ionizing radiation [7, 26]. Although rigorous testing of various protocols of amifostine administration is still required, the results of this study suggest for the first time that amifostine may be considered as preventive treatment for a wider spectrum of ALI syndromes associated with pathologic elevation of ROS production and oxidative stress (i.e. LPS-induced inflammation, ischemia/reperfusion).

Acknowledgements

This work was supported by grants from the ALA Carrier Investigator Award for KGB; NIH/NHLBI PO1-058064 for KGB and JGN; NIH/NCI RO1 CA99005 and DDE Grant DE-FG02-05ER64086 for DJG. The authors thank Nurgul Moldobaeva for superior technical assistance.

References

1.Bowie A, O'Neill LA. Oxidative stress and nuclear factor-kappaB activation: a reassessment of the evidence in the light of recent discoveries. *Biochem Pharmacol* 2000;59(1):13-23.

2.Tolando R, Jovanovic A, Brigelius-Flohe R, Ursini F, Maiorino M. Reactive oxygen species and proinflammatory cytokine signaling in endothelial cells: effect of selenium supplementation. *Free Radic Biol Med* 2000;28(6):979-86.

3.Haddad JJ, Land SC. Redox/ROS regulation of lipopolysaccharide-induced mitogen-activated protein kinase (MAPK) activation and MAPK-mediated TNF-alpha biosynthesis. *Br J Pharmacol* 2002;135(2):520-36.

4.Brizel DM, Wasserman TH, Henke M, Strnad V, Rudat V, Monnier A, et al. Phase III randomized trial of amifostine as a radioprotector in head and neck cancer. *J Clin Oncol* 2000;18(19):3339-45.

5.Murley JS, Kataoka Y, Hallahan DE, Roberts JC, Grdina DJ. Activation of NFkappaB and MnSOD gene expression by free radical scavengers in human microvascular endothelial cells. *Free Radic Biol Med* 2001;30(12):1426-39.

6.Nici L, Santos-Moore A, Kuhn C, Calabresi P. Modulation of bleomycin-induced pulmonary toxicity in the hamster by the antioxidant amifostine. *Cancer* 1998;83(9):2008-14.

7.Vujaskovic Z, Feng QF, Rabbani ZN, Samulski TV, Anscher MS, Brizel DM. Assessment of the protective effect of amifostine on radiation-induced pulmonary toxicity. *Exp Lung Res* 2002;28(7):577-90.

8.Nonas SA, Miller I, Kawkitinarong K, Chatchavalvanich S, Gorshkova I, Bochkov VN, et al. Oxidized phospholipids reduce vascular leak and

inflammation in rat model of acute lung injury. *Am J Respir Crit Care Med* 2006;173(10):1130-8.

9.Moitra J, Sammani S, Garcia JG. Re-evaluation of Evans Blue dye as a marker of albumin clearance in murine models of acute lung injury. *Transl Res* 2007;150(4):253-65.

10.Grdina DJ, Shigematsu N, Dale P, Newton GL, Aguilera JA, Fahey RC. Thiol and disulfide metabolites of the radiation protector and potential chemopreventive agent WR-2721 are linked to both its anti-cytotoxic and anti-mutagenic mechanisms of action. *Carcinogenesis* 1995;16(4):767-74.

11.Khawli FA, Reid MB. N-acetylcysteine depresses contractile function and inhibits fatigue of diaphragm in vitro. *J Appl Physiol* 1994;77(1):317-24.

12.Tsai JC, Jain M, Hsieh CM, Lee WS, Yoshizumi M, Patterson C, et al. Induction of apoptosis by pyrrolidinedithiocarbamate and N-acetylcysteine in vascular smooth muscle cells. *J Biol Chem* 1996;271(7):3667-70.

13.Birukova AA, Fu P, Chatchavalvanich S, Burdette D, Oskolkova O, Bochkov VN, et al. Polar head groups are important for barrier protective effects of oxidized phospholipids on pulmonary endothelium. *Am J Physiol Lung Cell Mol Physiol* 2007;292(4):L924-35.

14.Essler M, Amano M, Kruse HJ, Kaibuchi K, Weber PC, Aepfelbacher M. Thrombin inactivates myosin light chain phosphatase via Rho and its target Rho kinase in human endothelial cells. *J Biol Chem* 1998;273(34):21867-74.

15.Beckman JS, Koppenol WH. Nitric oxide, superoxide, and peroxynitrite: the good, the bad, and ugly. *Am J Physiol* 1996;271(5 Pt 1):C1424-37.

16.Gole MD, Souza JM, Choi I, Hertkorn C, Malcolm S, Foust RF, III, et al. Plasma proteins modified by tyrosine nitration in acute respiratory distress syndrome. *Am J Physiol Lung Cell Mol Physiol* 2000;278(5):L961-967.

17.Chen K, Keaney J. Reactive oxygen species-mediated signal transduction in the endothelium. *Endothelium* 2004;11(2):109-21.

18.Jones SA, Richards PJ, Scheller J, Rose-John S. IL-6 transsignaling: the in vivo consequences. *J Interferon Cytokine Res* 2005;25(5):241-53.

19.Kao SJ, Wang D, Lin HI, Chen HI. N-acetylcysteine abrogates acute lung injury induced by endotoxin. *Clin Exp Pharmacol Physiol* 2006;33(1-2):33-40.

20.Hashimoto S, Gon Y, Matsumoto K, Takeshita I, Horie T. N-acetylcysteine attenuates TNF-alpha-induced p38 MAP kinase activation and p38 MAP kinase-mediated IL-8 production by human pulmonary vascular endothelial cells. *Br J Pharmacol* 2001;132(1):270-6.

21.Behr J, Degenkolb B, Krombach F, Vogelmeier C. Intracellular glutathione and bronchoalveolar cells in fibrosing alveolitis: effects of N-acetylcysteine. *Eur Respir J* 2002;19(5):906-11.

22.Ahola T, Lapatto R, Raivio KO, Selander B, Stigson L, Jonsson B, et al. N-acetylcysteine does not prevent bronchopulmonary dysplasia in immature infants: a randomized controlled trial. *J Pediatr* 2003;143(6):713-9.

23.Bachy CM, Fazenbaker CA, Kifle G, McCarthy MP, Cassatt DR. Tissue levels of WR-1065, the active metabolite of amifostine (Ethyol), are equivalent following intravenous or subcutaneous administration in cynomolgus monkeys. *Oncology* 2004;67(3-4):187-93.

24.Elas M, Parasca A, Grdina DJ, Halpern HJ. Oral administration is as effective as intraperitoneal administration of amifostine in decreasing nitroxide EPR signal decay in vivo. *Biochim Biophys Acta* 2003;1637(2):151-5.

25.Spencer CM, Goa KL. Amifostine. A review of its pharmacodynamic and pharmacokinetic properties, and therapeutic potential as a radioprotector and cytotoxic chemoprotector. *Drugs* 1995;50(6):1001-31.

26.Grdina DJ, Murley JS, Kataoka Y. Radioprotectants: current status and new directions. *Oncology* 2002;63 Suppl 2:2-10.

27.Murley JS, Kataoka Y, Cao D, Li JJ, Oberley LW, Grdina DJ. Delayed radioprotection by NFkappaB-mediated induction of Sod2 (MnSOD) in SA-NH tumor cells after exposure to clinically used thiol-containing drugs. *Radiat Res* 2004;162(5):536-46.

28.Walton KA, Cole AL, Yeh M, Subbanagounder G, Krutzik SR, Modlin RL, et al. Specific phospholipid oxidation products inhibit ligand activation of toll-like receptors 4 and 2. *Arterioscler Thromb Vasc Biol* 2003;23(7):1197-203.

Figure Legends

Figure 1. Effect of amifostine on H_2O_2, LPS and IL-6-induced endothelial barrier dysfunction. Human pulmonary EC were grown on microelectrodes. **A -** At the time point indicated by first arrow, cells were pretreated with WR-1065 (0.4 mM, 1 mM or 4 mM, 30 min) followed by stimulation with H_2O_2 (250 mM) (indicated by second arrow). **B and C -** EC were pretreated with WR-1065 (4 mM, 30 min) followed by stimulation with LPS (200 ng/ml) (**B**), or combination of IL-6 (25 ng/ml) and its soluble receptor (SR, 100 ng/ml) (**C**), and TER reflecting EC permeability changes was monitored over the time. Shown are pooled data from three independent experiments.

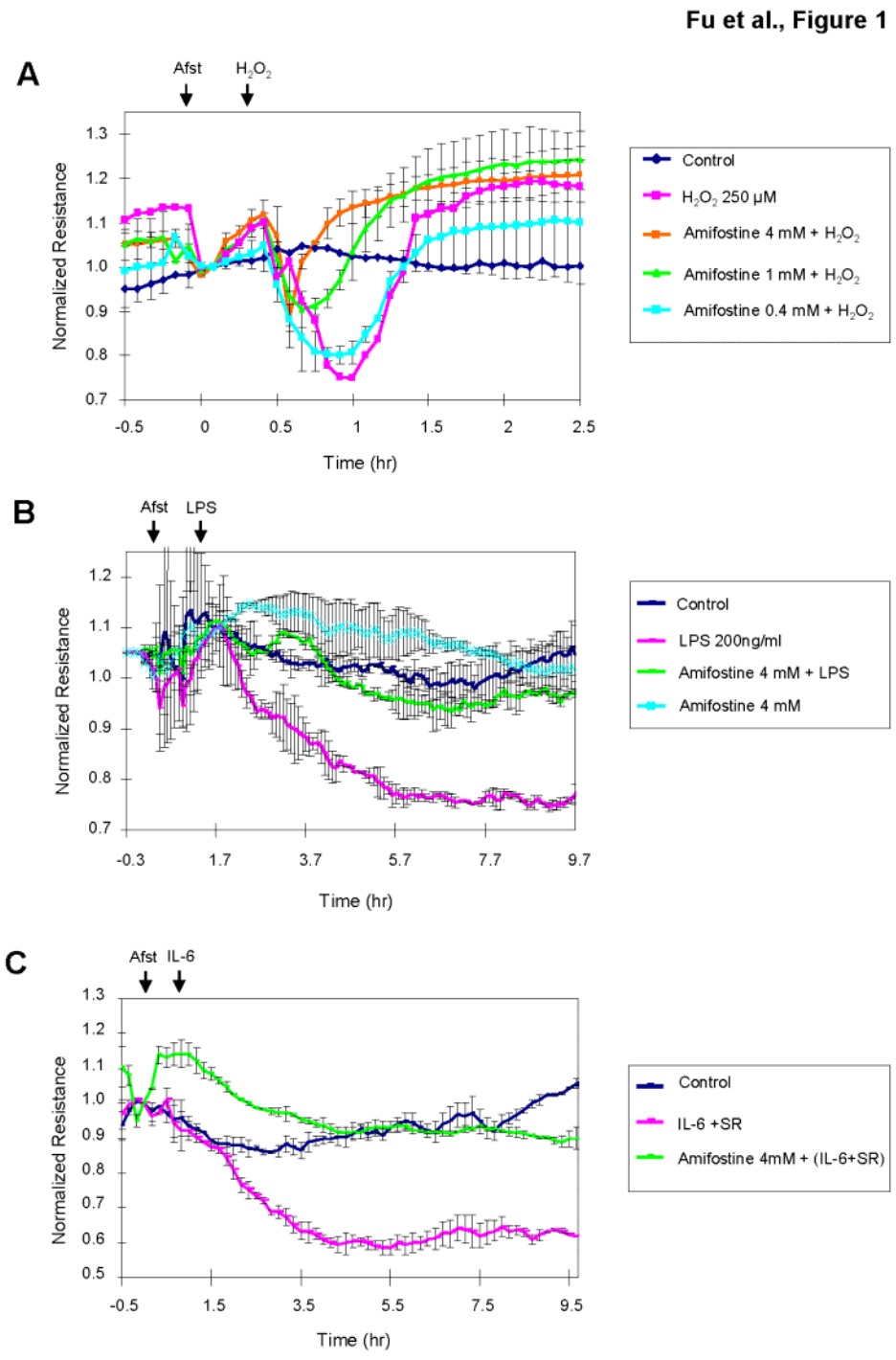

Figure 2. Amifostine prevents agonist-induced lung EC cytoskeletal remodeling and adherens junction disruption. EC grown on glass coverslips

were pretreated with amifostine (4 mM, 30 min) or vehicle followed by stimulation with H_2O_2 (250 mM, 15 min), LPS (200 ng/ml, 6 hrs), or IL-6 + SR (25 ng/ml and 100 ng/ml, 6 hrs). **A -** Actin cytoskeletal remodeling was assessed by immunofluorescence staining with Texas Red phalloidin. Paracellular gap formation is shown by arrows. **B -** VE-Cadherin staining was performed to visualize adherens junctions. LPS-induced disruption of adherens junctions is shown by arrows. The panels are representative of the entire cell monolayer. Shown are results of three independent experiments.

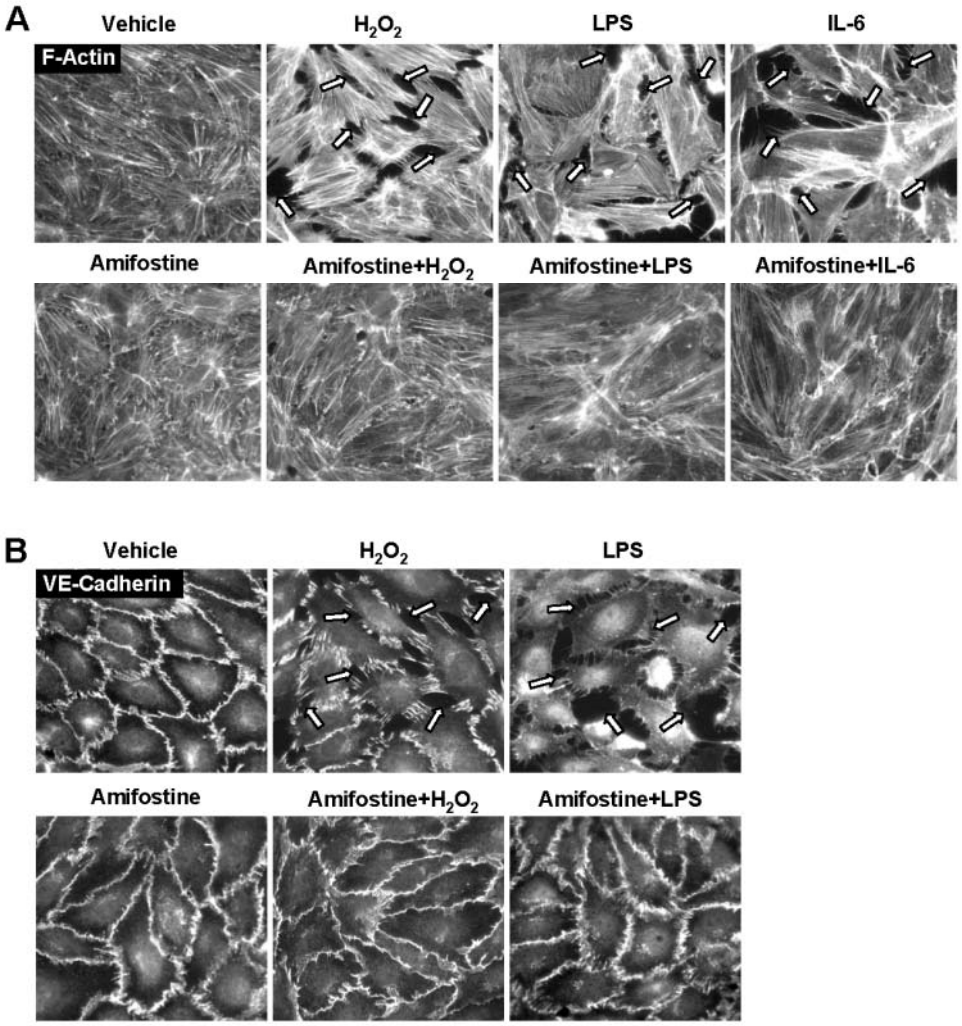

Figure 3. Amifostine inhibits ROS production induced by LPS. HPAEC were pretreated with vehicle (**top row**), NAC (5 mM, 1 h) (**middle row**) or WR-

1065 (4 mM, 30 min) (**bottom row**) followed by LPS stimulation (100 ng/ml, 200 ng/ml, or 500 ng/ml, 6 hrs). ROS was detected by DCFDA fluorescent assay described in the “Material and Methods”. The results are representative of the entire cell monolayer and have been reproduced in three independent experiments. **B -** Statistic analysis of the effect of NAC and amifostine on LPS-induced ROS production. * $p<0.005$, compared with NAC or amifostine pretreated EC. $^{\#}$ $P<0.05$, compared with 500 ng/ml LPS treated EC.

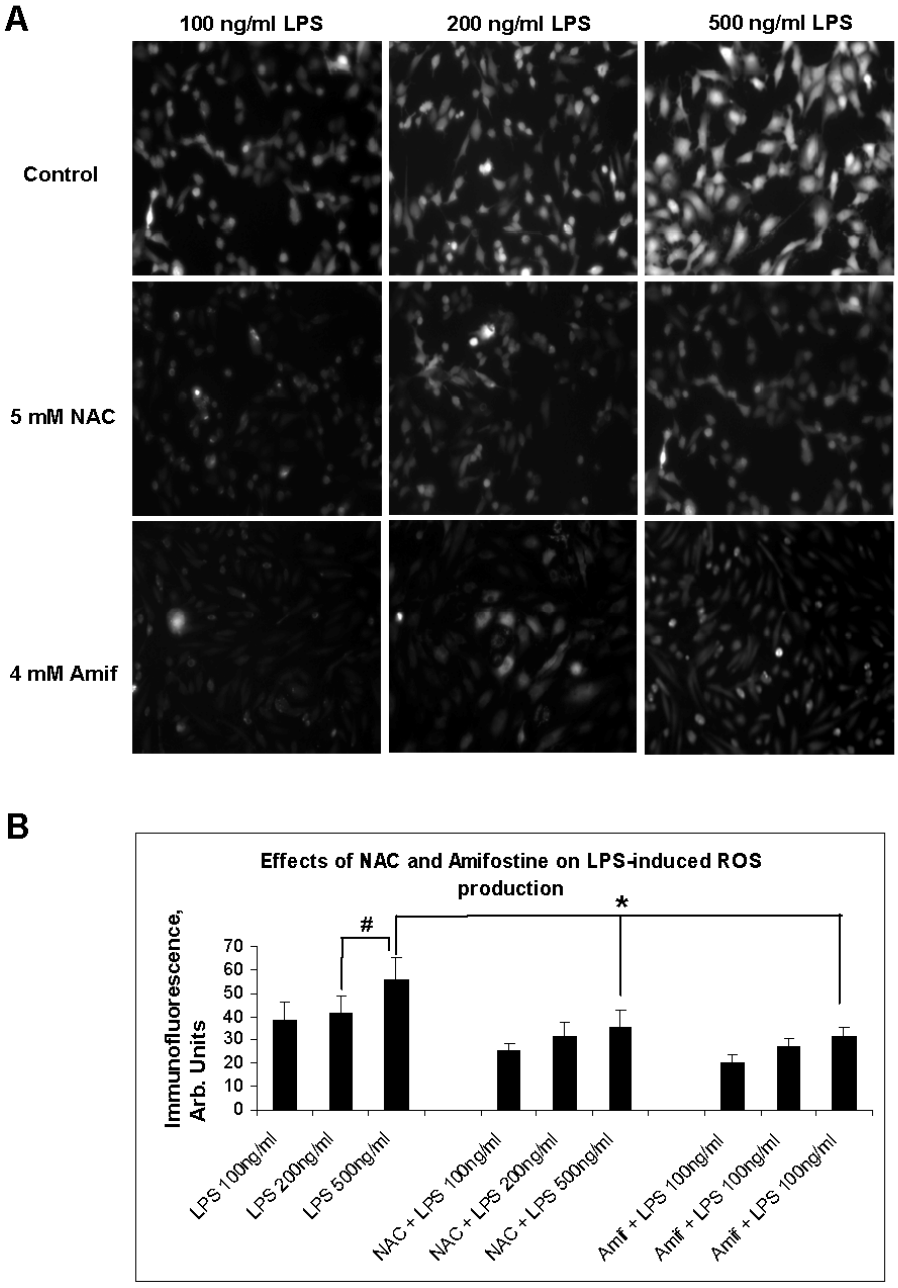

Figure 4. Amifostine attenuates intracellular signaling activated by inflammatory agonists. HPAEC were pretreated with amifostine (4 mM, 30 min) or vehicle followed by stimulation with: **A -** LPS (200 ng/ml, 2 hrs); **B -**

H_2O_2 (250 mM, 15 min); or **C -** IL-6 + SR (25 ng/ml and 100 ng/ml, 2 hrs). Phosphorylation of p38, MEK1/2, Erk1/2, IκBα, NκB-p65, MLC, and Hsp27 was detected with corresponding phospho-specific antibodies. Results are representative of three independent experiments.

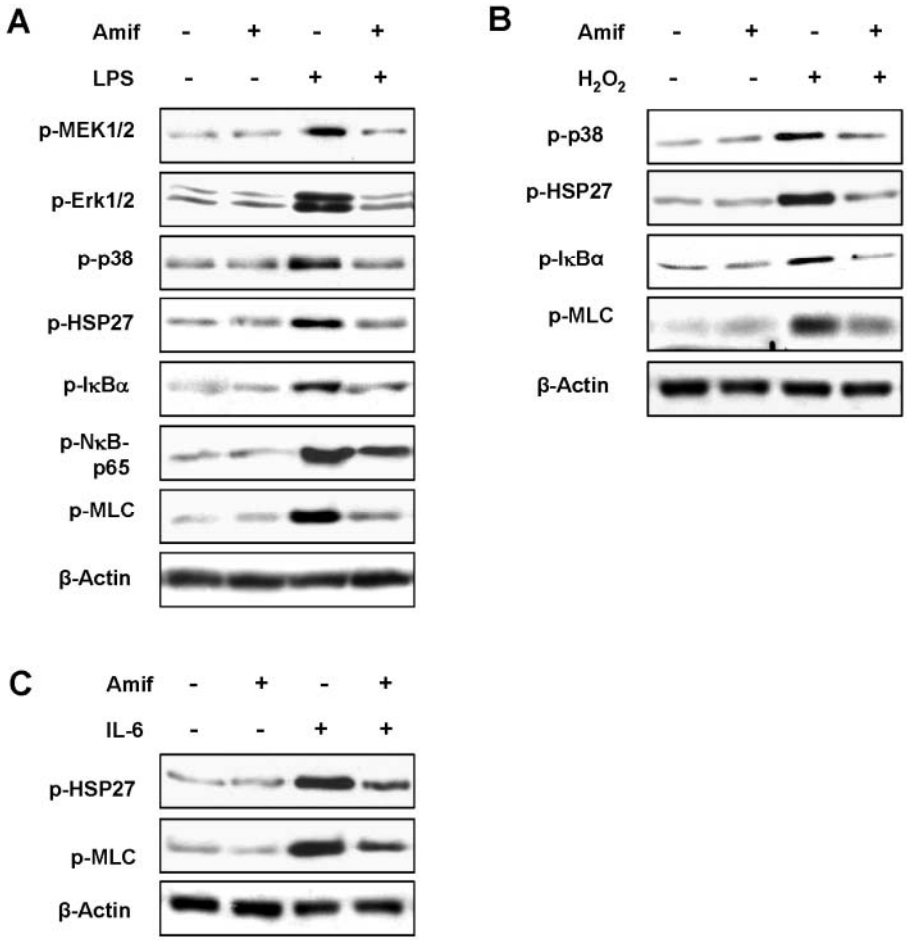

Figure 5. Amifostine attenuates LPS-induced neutrophil infiltration increased MPO activity. C57BL/6J mice were treated with LPS (0.7 mg/kg),

with or without concurrent treatment with WR-2721 (200 mg/kg) for 18 hrs. Control animals were treated with sterile water or WR-2721 (200 mg/kg) alone. **A and B -** After stimulation, cell count (**A**) and MPO activity (**B**) were measured in bronchoalveolar lavage fluid taken from control and experimental animals. (*p < 0.001 vs. control; **p < 0.001 vs. LPS; n=6-9 per group). **C -** Lungs were excised, fixed in 4% paraformaldehyde, embedded in paraffin, and used for histochemical analysis after hematoxylin and eosin staining. Images are representative of 6-9 lung specimens for each condition.

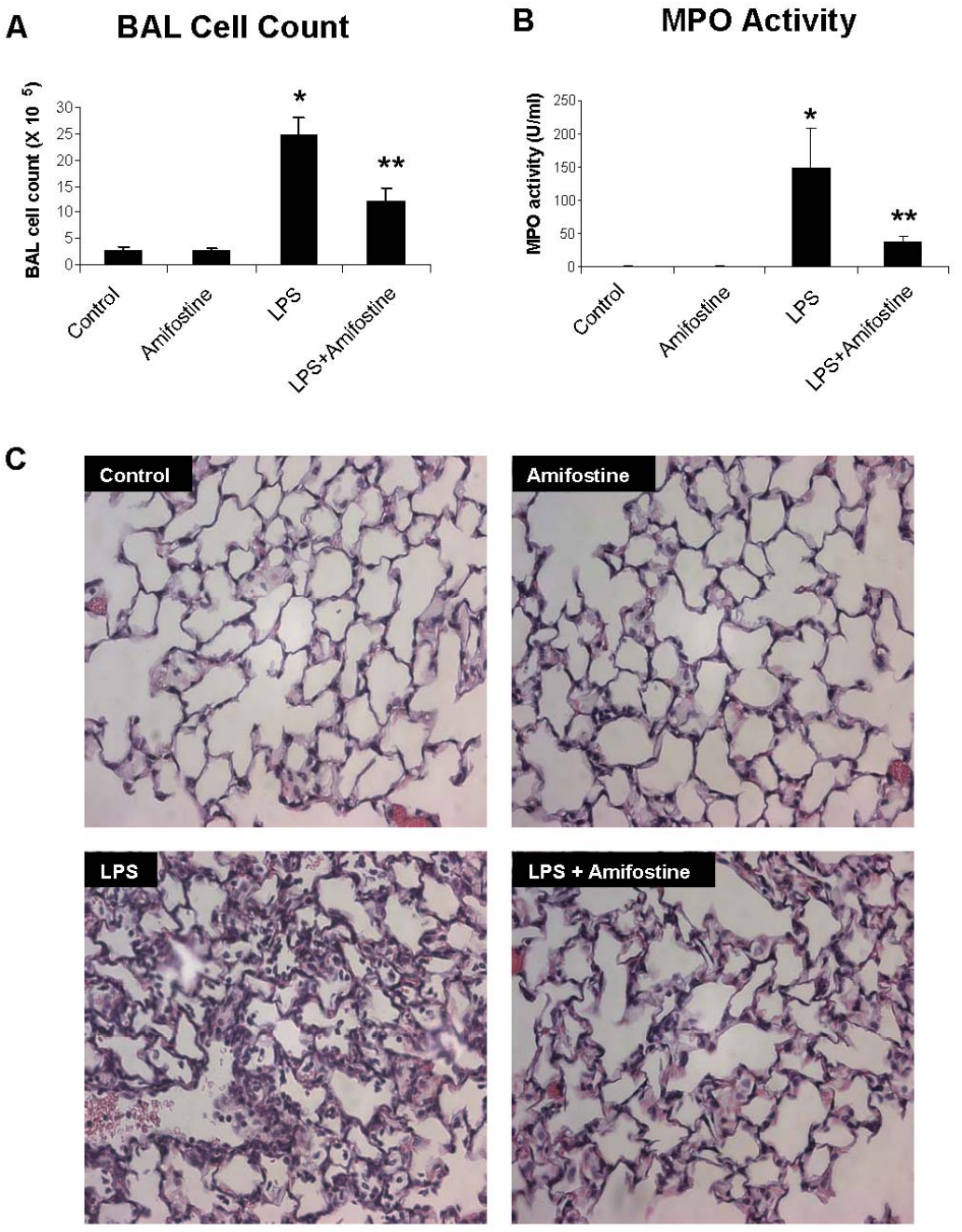

Figure 6. Amifostine attenuates LPS-induced lung vascular leak. C57BL/6J mice were treated with LPS (0.7 mg/kg), with or without concurrent treatment

with WR-2721 (200 mg/kg) for 18 hrs. Control animals were treated with sterile water or WR-2721 (200 mg/kg) alone. **A –** Protein concentration was measured in bronchoalveolar lavage fluid taken from control and experimental animals. **B and C -** Lung vascular permeability was assessed by Evans blue accumulation in the lungs as described in the “Materials and Methods”. **(B):** Images of the lungs represent Evans blue leakage into lung tissue. Results are representative of three independent experiments. **(C):** Quantitative spectrophotomertic analysis of Evans blue-labeled albumin extravasation. (*$p < 0.001$ vs. control; **$p < 0.001$ vs. LPS; n=3 per group).

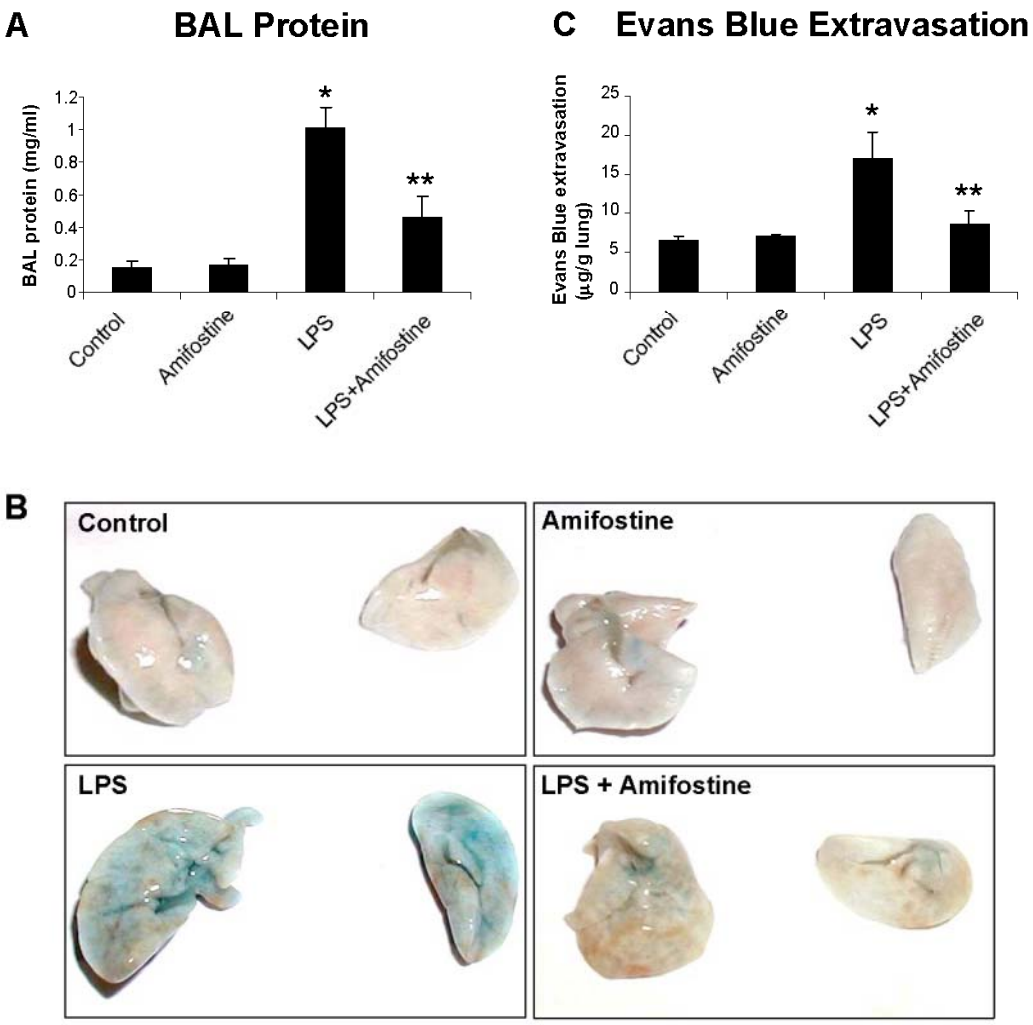

Figure 7. Amifostine inhibits LPS-induced oxidative stress-sensitive signaling in mouse lungs. A - C57BL/6J mice were treated with LPS (0.7

mg/kg), with or without concurrent treatment with WR-2721 (200 mg/kg). Control animals were treated with sterile water or WR-2721 (200 mg/kg) alone. Mouse lungs were harvested after 2 hrs or 6 hrs of LPS instillation, and tissue samples were prepared for western blot analysis. Accumulation of nitrotyrosinated proteins and p38 MAPK phosphorylation was detected using specific antibodies. Equal protein loading was confirmed by re-probing of membranes with β-actin antibodies. Results are representative of three independent experiments, * $p<0.005$. **B and C -** Dose dependence of amifostine effects on LPS-induced neutrophil accumulation and protein content in BAL. Mice were treated with LPS (0.7 mg/kg), with or without concurrent treatment with the range of WR-2721 doses (25 - 200 mg/kg). After 18 hrs of stimulation, cell count (**B**) and protein concentration (**C**) were measured in bronchoalveolar lavage fluid taken from control and experimental animals. (*$p < 0.001$ vs. control; **$p < 0.001$ 100 mg/kg vs. 200 mg/kg WR-2721; n=6-9 per group).

Fu et al., Figure 7A

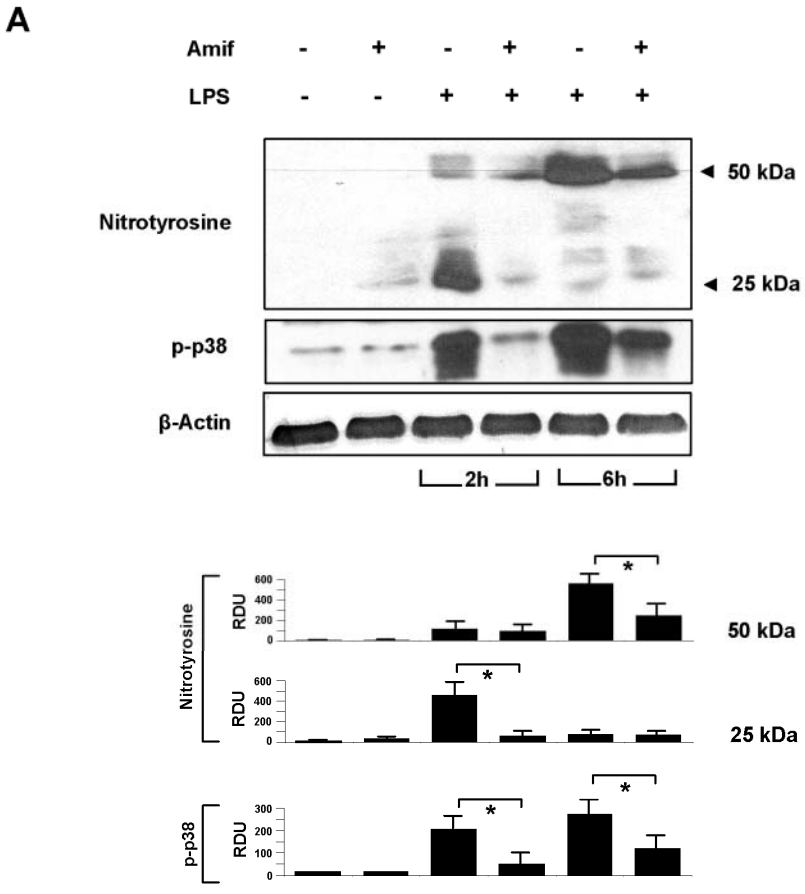

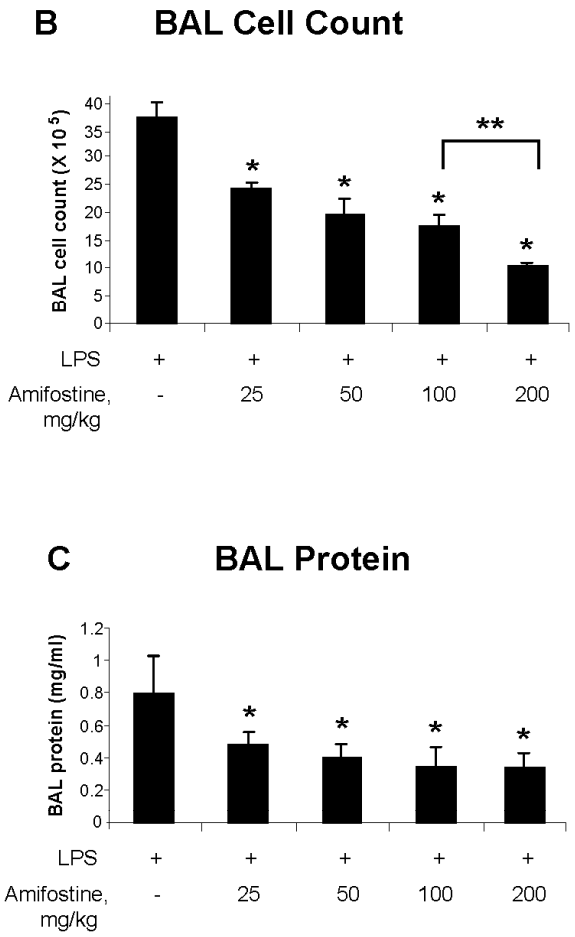

Figure 8. Inhibition of LPS-induced inflammation and endothelial barrier dysfunction by amifostine. Lung exposure to LPS results in activation of TLR4

receptor via LPS binding with LPS binding protein (LBP) and phosphatidylinositol glycan-linked cell surface protein, CD14. Subsequently, the LPS-CD14 complex interacts with toll-like receptor 4 (TLR4) and its accessory protein MD2. Alternative pathway of LPS-induced signaling may involve caveolae [28]. LPS signaling complex is assembled in caveolae, and the intracellular adaptor protein MyD88 and MAL are recruited to the Toll/IL-1 receptor cytoplasmic domain of TLR4 leading to activation of TLR-mediated signaling. LPS stimulates production of reactive oxygen and nitrogen species (ROS and RNS) by activating NADPH oxidase, NO-synthase, xanthine oxidoreductase and other enzymes, which leads to cellular oxidative stress. As a result, activation of redox-sensitive signaling cascades including NFkB, Erk-1,2 and p38 MAP kinases triggers cellular responses to LPS such as elevated expression of pro-inflammatory cytokines, cytoskeletal remodeling and disruption of endothelial monolayer integrity leading to acute lung injury. Amifostine reduces LPS-induced inflammatory signaling via inactivation of ROS and RNS and blunting the redox-sensitive inflammatory signaling.

Fu et al., Figure 8